Peer-reviewed version available at *Sensors* **2018**, *18*, 4393; doi:10.3390/s18124393

# All-fiber $CO_2$ sensor using Hollow Core PCF operating in the 2 μm region

**Sully M. M. Quintero[a], Luiz C. G. Valente[b], Marcos S. P. Gomes[a], Hugo G. da Silva[a] and Bernardo C. de Souza[a].**

[a] Mechanical Engineering Department, Pontifical Catholic University of Rio de Janeiro, Rua Marquês de São Vicente 225, 22453-900, Rio de Janeiro, RJ, Brazil; PUC-Rio: mspgomes@puc-rio.br; hugomes@puc-rio.br; bcarolid@aluno.puc-rio.br.

[b] Ouro Negro SA, Rua General Argolo 61, 20921-394, Rio de Janeiro, RJ, Brazil: luiz.guedes@ouronegro.com.br

*Correspondence: sully@puc-rio.br; Tel.: +55 21 3527 2800.

**Abstract**: A realistic implementation of an all-fiber $CO_2$ sensor, using 74 cm of hollow core PCF fiber as the cavity for light/gas interaction, has been implemented. It is based on CO2 absorbance in the 2μm region. The working range is from 2% to 100% $CO_2$ concentration at 1 atm total pressure. The response time obtained was 10 min. The use of an FBG tuned fiber ring laser, specifically designed for this application, is discussed and preliminary results with this laser are also presented.

**Keywords:** Gas sensor; photonic crystal fiber; tunable laser; fiber Bragg Grating; carbon dioxide monitoring

## 1 Introduction

Industrial applications for gas sensing technologies frequently require the sensing system to be immune to interference, to resist to a harsh environment, to be safe regarding the risk of fires and explosions, and the sensors are often installed in such a way that the communication between them and the recording equipment cannot be processed in a wireless mode. For example, in the oil industry, the measurement of carbon dioxide concentrations in carbon capture and geologic storage operations (CCS) may require the sensor to be installed deep in a $CO_2$ injection well, or inside a surface oil-gas separation equipment working in high pressures, creating great difficulties with respect to the transmission of the sensor signal. The same restrictions may apply to other situations of practical interest to several industries, in which fiber optic sensors may be selected as the more appropriate option. Qiao et al. (2017) calls the attention for the necessity of the oil and gas industry with respect to advances in technology for cost-effective production in new areas [1]. Applications are described for fiber Bragg gratings (FBGs) sensors in the well-logging field, including seismic explorations. The environment in which the sensors have to perform is extremely severe, and the advantages of using fiber optic sensors in such circumstances are enumerated in comparison with other types of technologies.

Fiber optic sensors are less prone to interference, and, depending on the wavelength used, the fiber provides an efficient way to communicate the signal at distances of several kilometers. In principle, it can be compact and light weight and it does not require electric power near measurement location. For gas measurement several spectroscopic techniques can be adapted using fiber to guide light to the measurement location such as Raman, absorbance and interference. Hollow-Core Photonic Crystal Fibers (HC-PCF) present attractive promises for the

implementation of these techniques as it provides excellent overlap of light and gas inside its hollow core with long interaction length with reduced size and weight.

Several authors have demonstrated many configuration using microstructure fibers for gas detection [2]. Cubillas et al. [3] demonstrated a HC-PCF as a gas cell for methane detection at 1.3 um. An investigation about the feasibility of using microestructured fiber in acetylene gas detection in the 1.5 um region was reported by Ritari et al. [4]. Yang et al. [5] describes a Raman spectroscopy system for the detection of several gases, including carbon dioxide, and vapors, using a HC-PCF probe for gas sensing in environmental control applications. Heidari et al. [6] describes a miniaturized microstructure spectroscopic gas sensor using a tunable slow-light hollow core photonic crystal fiber, and call the attention for the enhanced electrical field, localized in the hollow-core of the fiber, due to tunability of slow-light modes. Other approaches have also been implemented, exploring photonic crystal fibers Villatoro et al. [7] demonstrated a PCF interferometer system for chemical vapor detection. Nevertheless HC-PCF has drawbacks that have prevented the use in commercial sensing systems. Among these problems are the difficulty of efficiently coupling light and gas to its core, the long response time and the presence of unstable guided high order modes [8].

In this work a complete, rugged all-fiber system that allow $CO_2$ measurement in a wide concentration range (2% to 100%) at atmospheric pressure is presented. Using lasers with output power on the order of 1W it is possible to reach distances of more than 1km from measurement point. Absorbance measurement is a linear optical property that can be easily implemented and is immune to absolute power fluctuations. When selecting the wavelength of to be used to sense $CO_2$ in a fiber optic system one has to consider several aspects as the interaction length, in this case the HC-PCF length, the total optical fiber length and the absorption intensity. Figure 1 shows the light transmittance across 74 cm of $CO_2$ at 20% concentration and total pressure of 1 atm. At 1.58 µm, telecom fibers present extremely low attenuation and all optical components are readly available but the weak lines would demand a long interaction length. Other options are to explore the absorption lines near 1.95 µm and 2.0 µm. Conventional $SiO_2$ based fibers present attenuation that increases steeply beyond 1.8 µm reaching 10 dB/km at 1.95 µm 20 dB/km at 2.0 µm [9][10]. The choice between these two wavelength regions will depend on the specific application, including distance of operation and optical power of the interrogator.

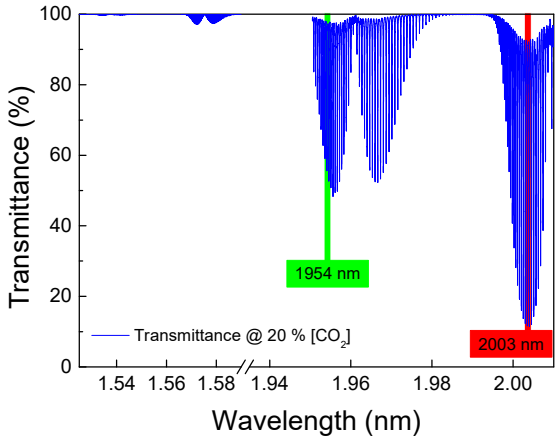


**Figure 1.** Transmittance for 20% CO2 concentration and total pressure of 1atm in a 74cm optical path

## 2 Sensor Design and FBG tuned laser

### *2.1 Sensor Design*

The working principle of this sensor is the measurement of the transmittance of light, through a certain length of HC-PCF (NKT HC 2000). The spectrum of the light is continuously scanned around the wavelength of a predetermined absorption line of $CO_2$. As depicted in Figure 2, light is launched in the HC-PCF from a single mode fiber (SMF 28) and collected with a multi mode fiber. In both sides a gap of few microns allow the gas to enter the sensing region.The gas inlet and outlet are placed inside small boxes, specially designed to accommodate an alignment base. It is hermetically sealed with a connection for a tube through which a remote, small pumping system maintains a negative pressure at the outlet side to force the gas into the HC-PCF. This scheme reduces the response time of the sensor to 10 min, as can be seen in the results presented in Figure 7 in the next section.

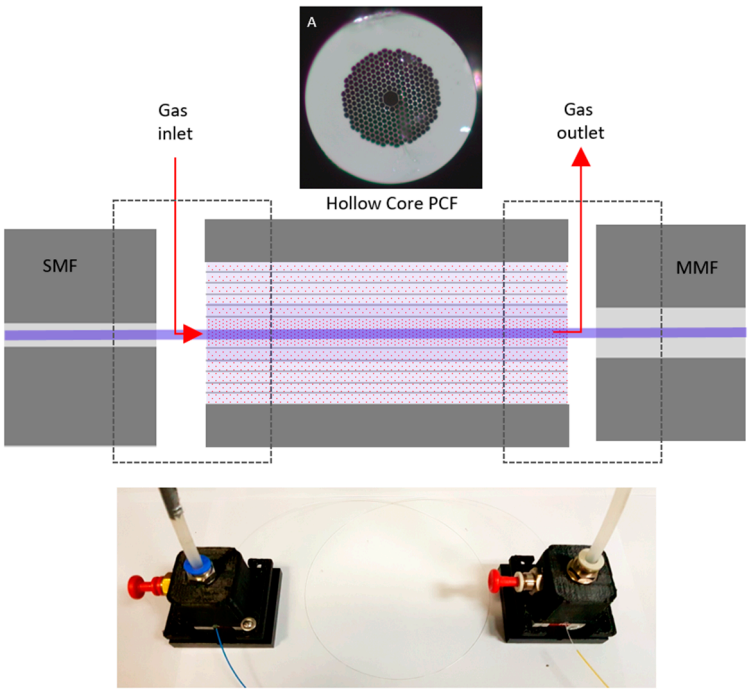


**Figure 2.** Schematic representation and photograph of the devices used to inject and extract gas and light from the sensing HCPCF. In detailthe cross section of the HCPCF used.

A schematic view of the complete system is presented in Figure 3, as can be seen, the laser light is split in two arms, one used as a power reference while the other carries light to the sensing unit presented in Figure 2. This system can be used with different lasers, addressing any of the spectral regions of interest.

In Figure 4 a simulation of the transmittance using Hitran for a 74 cm long cavity as function of the $CO_2$ concentration for three different wavelengths (1,954.5nm, 1,997.0nm and 2,003.5nm) [11]. For concentrations below 20%, the 2,003.5 line is the best choice but it saturates at higher concentrations and, for higher concentration levels, the system must be operated either at 1,997.0nmor at 1,954.5nm. These lines were choosed based on their strength and the absence of water vapor lines in its vicinity.

Depending on which wavelength the laser is operating, the processing unit compares the measured transmittance to the appropriate curve to calculate the CO2 concentration. It is

Preprints (www.preprints.org) | NOT PEER-REVIEWED | Posted: 31 October 2018 doi:10.20944/preprints201810.0747.v1

Peer-reviewed version available at Sensors 2018, 18, 4393; doi:10.3390/s18124393

important to point that the working principle of this implementation does not require any calibration, making it very stable and not influenced by variations in absolute power level.

The laser used to obtain the results presented in the next section was a Single-Frequency Tunable $Cr^{2+}$:ZnS/Se Laser from IPG, with output power up to 2W. It´s spectral linewidth is 0.7 MHz and the tuning range adjustable from 1,933 nm to 2,245nm. The scanning speed can be selected between 0.04 nm/s and 35.70 nm/s.

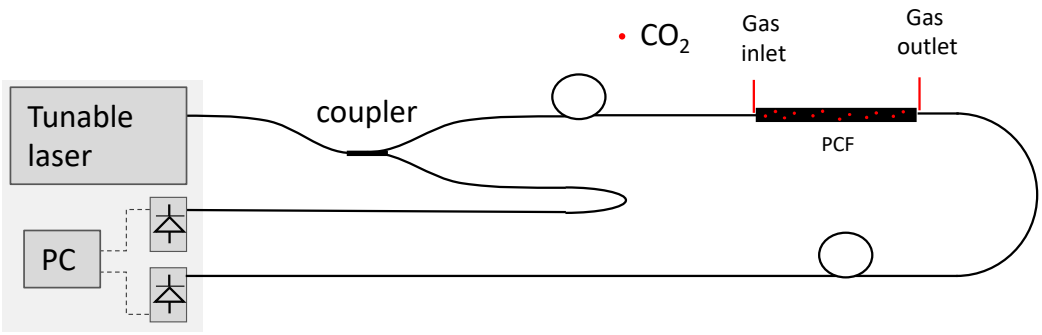


**Figure 3.** Complete sensor schematic setup, including HC-PCF based gas/light interaction cavity and PC based acquisition and processing unit.

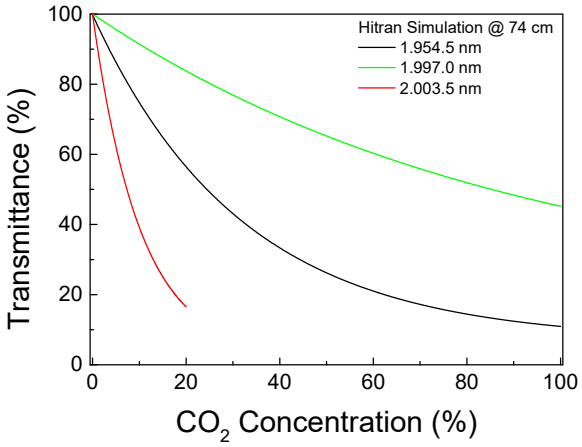


**Figure 4.** Transmittance across a 74cm long cavity at total pressure of 1 atm, as function of $CO_2$ concentration.

The acquisition and processing unit uses a NI 6009 DAC board[12], connected to a PC runing a program written in Labview. The program is responsible for all the digital control and processing, going from the DAC board settings, all the way to the users interface. Figure 5 shows the end user´s interface where information on $CO_2$ concentration history and optical signal can be visualized.

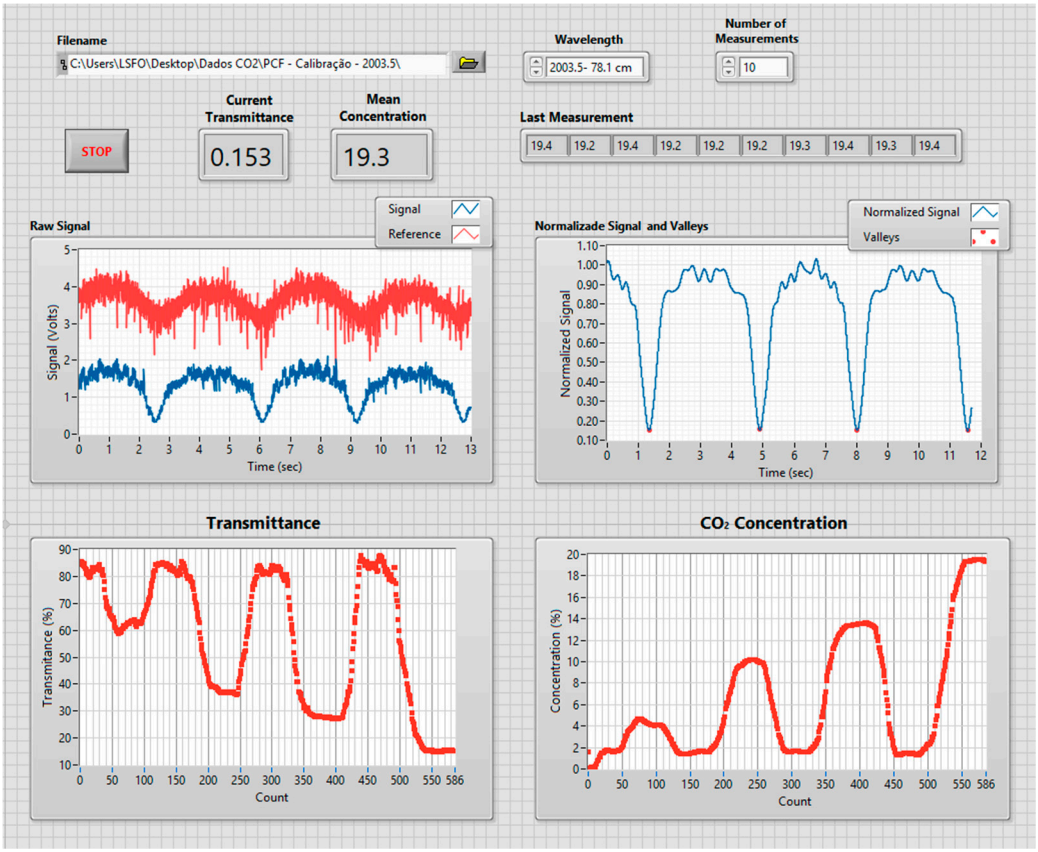


**Figure 5.** Computer interface of the acquisition and processing unit of the sensor

*2.2 FBG tuned laser*

Although the IPG laser used was totally satisfactory as a light source for this sensor, it is an expensive and large piece of equipment. Looking to future field applications, a compact, low cost all fiber tunable laser is under development. For the intended application, it is desired that the tuning range can be adjusted from a few nm to several tens of nm. The freedom to choose the center of the tuning range is very important to allow the use of different $CO_2$ absorption lines.

The schematic setup of this laser is presented in Figure 6. It is based in a commercial optical fiber amplifier with a useful gain curve spreading from 1.940nm to 2.010nm. The laser feedback is given by an FBG whose reflection peak is mechanically controlled to tune the output wavelength of the laser. FBGs can be elongated or compressed in excess to +/- 2.5% (100 nm in this case) of spectral excursion without damage [13], which allows to cover all the desired spectral region. The output power of this laser is dictated by the 2μTm fiber amplifier which, in this AP-AMP1 [14] is 140mW. Figure 6 also shows the power and wavelength stability of this laser which is still under final adjustments.

Preprints (www.preprints.org) | NOT PEER-REVIEWED | Posted: 31 October 2018 doi:10.20944/preprints201810.0747.v1

Peer-reviewed version available at Sensors 2018, 18, 4393; doi:10.3390/s18124393

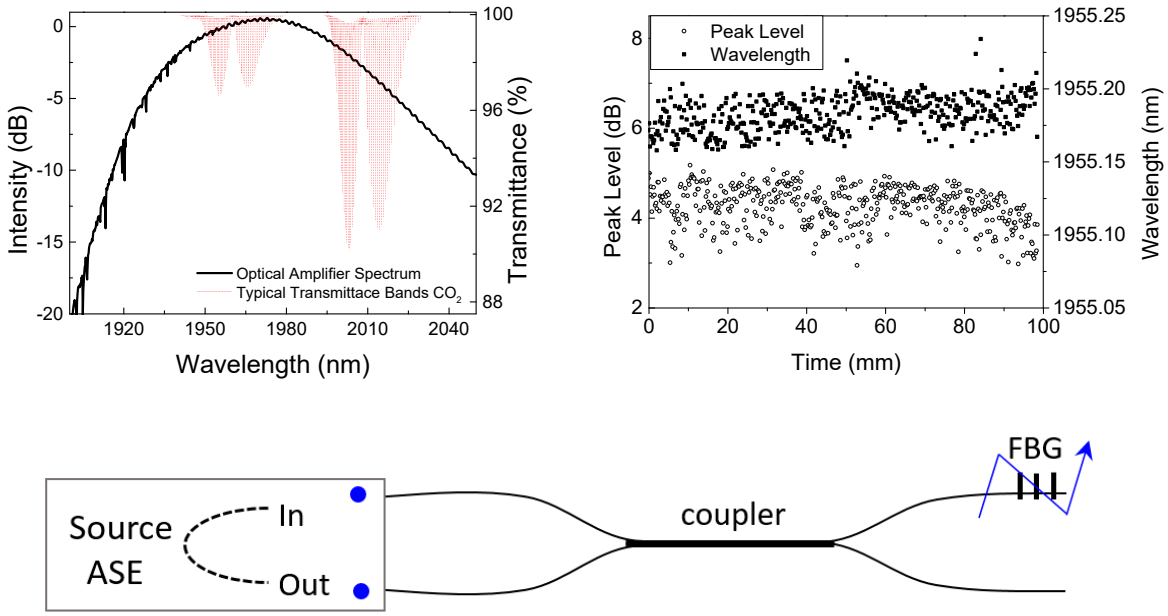


**Figure 6.** Schematic diagram of the FBG tuned laser. Insets show Fiber amplifier gain curve and wavelength and power stability.

## 4. Results and Discussion

The system is extremely flexible and, depending on the specific application, some operational parameters can be changed to achieve the best performance. For the results presented in this section, the following parameters were used.

Wavelength span: 0.6 nm (2003.1nm to 2003.7nm)
Sweep speed: 0.2nm/s
Measurement update interval: 12s

With these settings, every 12s the system reads 4 times the same absorption line and processes it presenting the average transmittance at maximum attenuation. Individually, each of the 4 measurements correspond a trace similar to those shown in Figure 7. These measurements are converted to CO2 concentration and shown in the user´s interface panel. The system offers an option of continuously averaging a number of measured points, which can be choosed by the user. The latest value, as well as the CO2 concentration history, is presented to the user. As a default, the system saves all raw data obtained which, if necessary, can later be reprocessed with different settings.

In order to characterize the overall sensor's performance when exposed to different $CO_2$ concentrations, it was exposed to cycles of pure $N_2$ and 5%, 10%, 15% and 20% of $CO_2$. Figure 8 shows the transmittance at the 2,003.5nm during these gas cycles. As observed during these cycles, the response time of the system was approximately 10min. As can be seen, in the typical signal shown in Figure 7, non fundamental modes introduce a signal background fluctuation with spectral frequency that can not be separated from the optical signal of interest. The amplitude of these fluctuations is on the order of 10% of the total signal, which translates into, approximately, 1.5% of $CO_2$ concentration when using the 2,003.5nm absorption line. This effect explains why the maximum transmittance level shown in Figure 8 is not 100% for pure $N_2$.

Preprints (www.preprints.org) | NOT PEER-REVIEWED | Posted: 31 October 2018 doi:10.20944/preprints201810.0747.v1

Peer-reviewed version available at Sensors 2018, 18, 4393; doi:10.3390/s18124393

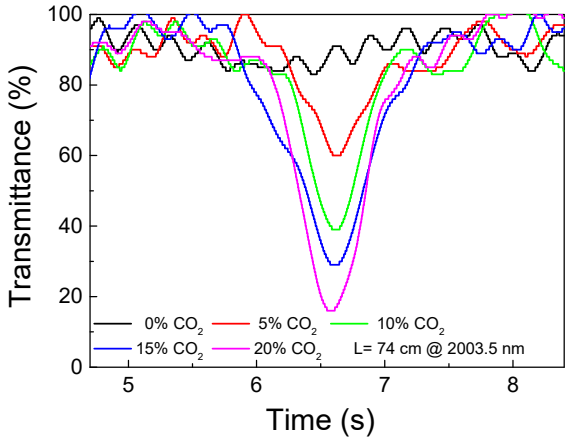


**Figure 7.** Typical normalized optical signal at different concentration levels.

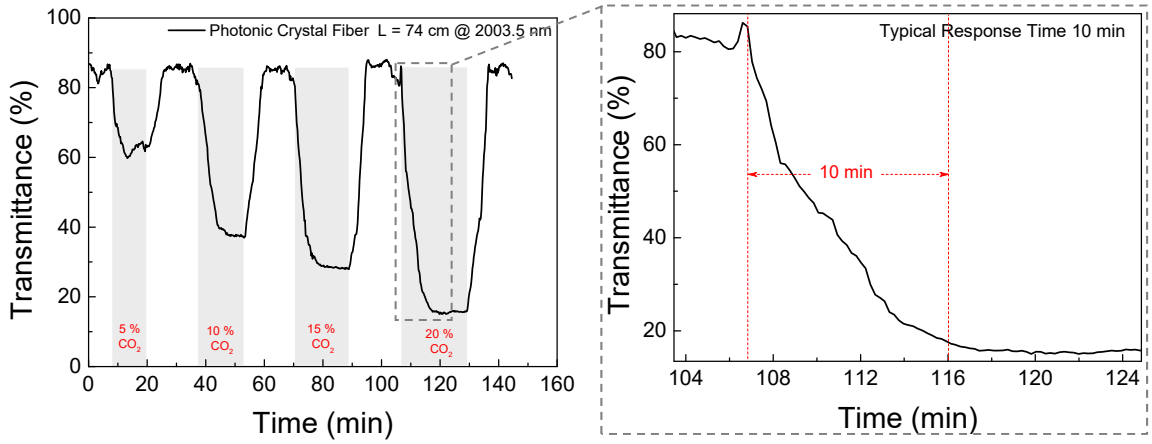


**Figure 8.** Transmittance measured for cycles of different $CO_2$ concentration (0%, 5%, 10%, 15% and 20%).

As mentioned earlier the processing software translates the measured transmittance into $CO_2$ concentration using curves shown in Figure 4. The final performance of the sensor can be appreciated in Figure 9, where its output is compared with the reference gas concentration. Measurements were performed at 2,003.5nm and 1,954,5nm for concentrations of up to 20% $CO_2$. The 1,997.0nm line was used for $CO_2$ concentrations of 20% and 100%.

The presence of higher order modes not only limit the minimum detectable $CO_2$ concentration but also introduces measurement uncertainties. Using an average of 10 points for each final measure, the mean error was 0,4% of $CO_2$ concentration with a maximum error was 0,7%.

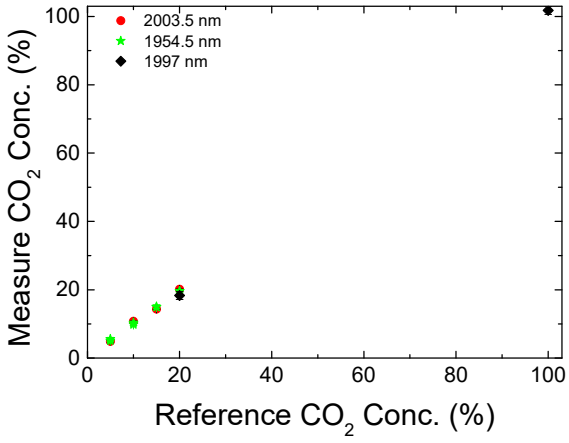


**Figure 9.** Final $CO_2$ concentration presented by the sensor compared with nominal concentration of the measured gas.

## 5 Conclusion

Due to it's all fiber configuration the sensing system presented is mechanically very stable, it's working principal makes it independent of recalibrations, suitable for long period applications. Even though the fiber attenuation is in the range of 10dB/km to 20dB/km, the high power of the light source used, enables applications at distances beyond 1km between the power source and the measurement point.

Although the accuracy of the sensor is better than 0.5% of $CO_2$ concentration, the presence of high order modes limit the minimum detectable $CO_2$ level to 2%. Without any significant change, but at the expense of increasing the response time, longer HC-PCF could be employed reducing the minimum detectable level. If improved fibers, with lower mode interference modes, were available the system would operate from ambient $CO_2$ levels all the way to pure $CO_2$.

**Acknowledgments:** This research was funded by Petrobras through the project TCBR 304

**Author Contributions:** S.M.M.Q., M.S.P.G and L.C.G.V. conceived the $CO_2$ sensor and performed the experiments; B.C assembled the experimental setup; and H.G.D.S. developed the processing code in Labview. All authors contributed to the writing of the manuscript.

**Conflicts of Interest:** The authors declare no conflict of interest.

## References

[1] X. Qiao, Z. Shao, W. Bao, and Q. Rong, "Fiber Bragg Grating Sensors for the Oil Industry," *Sensors*, vol. 17, no. 3, p. 429, Feb. 2017.

[2] P. S. Light, F. Couny, and F. Benabid, "Low optical insertion-loss and vacuum-pressure all-fiber acetylene cell based on hollow-core photonic crystal fiber," *Opt. Lett.*, vol. 31, no. 17, p. 2538, Sep. 2006.

[3] A. M. Cubillas, J. M. Lazaro, M. Silva-Lopez, O. M. Conde, M. N. Petrovich, and J. M.

Lopez-Higuera, "Methane sensing at 1300 nm band with hollow-core photonic bandgap fibre as gas cell," *Electron. Lett.*, vol. 44, no. 6, p. 403, 2008.

[4] T. Ritari *et al.*, "Gas sensing using air-guiding photonic bandgap fibers," *Opt. Express*, vol. 12, no. 17, p. 4080, Aug. 2004.

[5] X. Yang, A. S. P. Chang, B. Chen, C. Gu, and T. C. Bond, "High sensitivity gas sensing by Raman spectroscopy in photonic crystal fiber," *Sensors Actuators B Chem.*, vol. 176, pp. 64–68, Jan. 2013.

[6] M. Ebnali-Heidari, F. Koohi-Kamali, A. Ebnali-Heidari, M. K. Moravvej-Farshi, and B. T. Kuhlmey, "Designing Tunable Microstructure Spectroscopic Gas Sensor Using Optofluidic Hollow-Core Photonic Crystal Fiber," *IEEE J. Quantum Electron.*, vol. 50, no. 12, pp. 1–8, Dec. 2014.

[7] J. Villatoro *et al.*, "Photonic crystal fiber interferometer for chemical vapor detection with high sensitivity," *Opt. Express*, vol. 17, no. 3, p. 1447, Feb. 2009.

[8] S. Schilt, R. Matthey, K. Hey Tow, L. Thévenaz, and T. Südmeyer, "All-fiber versatile laser frequency reference at 2 μm for CO2 space-borne lidar applications," *CEAS Sp. J.*, vol. 9, no. 4, pp. 493–505, Dec. 2017.

[9] T. Izawa, N. Shibata, and A. Takeda, "Optical attenuation in pure and doped fused silica in the ir wavelength region," *Total Opt. Attenuation Bulk Fused Silica Appl. Phys. Lett.*, vol. 31, p. 264, 1977.

[10] L. B. Jeunhomme, *Single-mode fiber optics : principles and applications*. Marcel Dekker, 1990.

[11] L. S. Rothman *et al.*, "The HITRAN2012 molecular spectroscopic database," *J. Quant. Spectrosc. Radiat. Transf.*, vol. 130, pp. 4–50, 2013.

[12] "SPECIFICATIONS USB-6009." [Online]. Available: http://www.ni.com/pdf/manuals/375296c.pdf. [Accessed: 28-Oct-2018].

[13] "Products - Strain sensors - SG-01 | FBGS - Draw Tower Gratings." [Online]. Available: http://www.fbgs.com/products/strain-sensors/sg-01/. [Accessed: 12-Jul-2017].

[14] "AdValue Photonics - Fiber Amplifier." [Online]. Available: http://www.advaluephotonics.com/products/2-um-fiber-amplifiers/fiber-amplifier. [Accessed: 28-Oct-2018].